# Inverse scattering with singular potentials: A supersymmetric approach

J.-M. Sparenberg and D. Baye
*Physique Nucléaire Théorique et Physique Mathématique, C.P. 229, Université Libre de Bruxelles, Campus Plaine, B 1050 Brussels, Belgium*
(Received 16 December 1996)

By using potentials with a singularity at the origin, the inverse scattering problem at fixed orbital momentum $l$ can be decomposed in two parts. First, the unique singular potential without a bound state corresponding to a given phase shift is constructed; then, bound states may be added without modifying the phase shift. The first step, called the singular inverse problem, is discussed. When the phase shift is smaller at high energies than at zero energy, the obtained effective potential has a repulsive core of the form $\nu(\nu+1)r^{-2}$ where $\nu$ is larger than $l$. If the $S$ matrix can be approximated by the product of the $S$ matrix of a reference potential by a rational function of the wave number $k$, the singular potential is a generalized Bargmann potential. It can be constructed with supersymmetric transformations of the reference potential. Each transformation adds a pole to the $S$ matrix. The repulsive core parameter $\nu$ of the final potential is equal to $l$ plus the difference of the number of added poles in the upper and lower half $k$ planes. This generalized Bargmann potential as well as its solutions can be expressed in terms of the reference potential and of Wronskians of its solutions. As an application, we invert the phase shifts of neutron-proton and proton-proton $^1S_0$ elastic scatterings and obtain in both cases a $\nu=1$ singular nuclear potential with two wells. In the neutron-proton case, this potential is compared with a regular potential obtained from a Gel'fand-Levitan-Marchenko inversion method. [S0556-2813(97)00805-4]

PACS number(s): 03.65.Nk, 21.45.+v, 13.75.Cs

## I. INTRODUCTION

The standard approach to the inverse-scattering problem [1] at fixed orbital momentum only considers potentials which are ''regular'' at the origin, i.e., less singular than $r^{-2}$. In fact, if the Schrödinger equation of a given partial wave is considered as a one-dimensional problem, the corresponding *effective* potential is singular because of the centrifugal part of the kinetic energy, except for the $s$ wave. This effective potential $V(r)$ verifies

$$V(r) \underset{r\to 0}{\to} \frac{l(l+1)}{r^2}, \tag{1}$$

where $l$ is the orbital momentum. This well-known property apparently relates the singularity of the effective potential to the symmetry of the partial wave. At large distances, the Schrödinger equation must reproduce a free-particle or Coulomb motion. Therefore, the asymptotic $l(l+1)r^{-2}$ form of $V(r)$ for $r$ tending towards infinity is physically related to the partial wave $l$. However, this is not the case for the singularity of $V(r)$ at the origin. The distinction between regularity and singularity is not crucial for the resolution of the equation or for the calculation of scattering properties. We show below that using singular potentials, i.e., potentials which do not satisfy Eq. (1), opens new approaches for inverse scattering.

When the phase shift does not tend at high energies to its zero-energy value, inversion procedures with regular potentials require the introduction of $N$ bound states, where $N$ is related to the phase shift by the Levinson theorem: $\delta(0)-\delta(\infty)=N\pi$. Even when the $N$ bound-state energies are physically known, ambiguities occur in the inverse problem because $N$ arbitrary normalization constants are simultaneously introduced [2]. Moreover, in many cases [3], the difference between the zero- and infinite-energy phase shifts cannot be explained only with physical bound states. The remaining difference is due to the effect of the Pauli principle between composite particles: The phase-shift difference is related to the occurrence of a number of so-called ''forbidden states'' [4,5]. The inverse problem then becomes even more ambiguous because both the energy and normalization choices for the forbidden states are arbitrary.

In the supersymmetric approach applied to the construction of phase-equivalent potentials, ''singular'' potentials naturally appear when bound states are removed from a regular potential [6–10]. Near the origin, the corresponding effective potentials verify

$$V(r) \underset{r\to 0}{\to} \frac{\nu(\nu+1)}{r^2}, \tag{2}$$

where $\nu$ is an integer, larger than the orbital momentum. In many respects, these singular potentials do not behave differently from regular ones. However, the difference between the phase shifts at zero and infinite energies is related to $\nu$, through the generalized Levinson theorem [11]

$$\delta(0)-\delta(\infty)=[N+\tfrac{1}{2}(\nu-l)]\pi, \tag{3}$$

where $N$ is the number of remaining bound states of the potential. We have conjectured that this theorem remains valid even in the presence of a Coulomb interaction [12].

This theorem suggests a new approach to the inverse problem: From a phase shift at fixed $l$, it is always possible to determine a *singular* potential without any bound state.

 

The parameter of the singular repulsive core of this potential is, according to Eq. (3) with $N=0$,

$$\nu = l + \frac{2}{\pi}[\delta(0) - \delta(\infty)]. \tag{4}$$

Because of the lack of a bound state, this potential is unique. In the following, the problem of constructing this singular potential from the phase shift will be referred to as the *singular inverse problem*. The regular or traditional inverse problem can consequently be solved in two steps: (i) determining the solution of the singular inverse problem, which only depends on scattering data, and (ii) adding given bound states with given normalization constants to the spectrum without modifying the phase shifts.

As already shown in [10], *pairs* of supersymmetric transformations can perform step (ii). To our knowledge, step (i) has not been addressed yet. It can be performed with good accuracy by *single* supersymmetric transformations, as explained in this paper. Let us emphasize here that singular potentials can probably be obtained with slight modifications of other inversion methods. However, supersymmetry has various advantages: It is quite simple, it allows one to solve both the singular inverse problem and the addition of bound states, and it treats the Coulomb interaction without much additional complication.

In Sec. II, the principle of single supersymmetric transformations is recalled and the corresponding modifications of the $S$ matrix are studied. In Sec. III, the singular inverse problem is solved by iteration of supersymmetric transformations when the $S$ matrix is the product of a reference $S$ matrix by a rational function of the wave number. We then apply the method to the nucleon-nucleon $^1S_0$ elastic scattering in Sec. IV and conclude in Sec. V.

## II. SINGLE SUPERSYMMETRIC TRANSFORMATIONS

Let us first recall the principle of supersymmetric (or Darboux) transformations [13–15]. Consider a given Schrödinger equation at fixed orbital momentum $l$ for a complex wave number $k$ (in units $\hbar = 2\mu = 1$, where $\mu$ is the reduced mass of the system),

$$H_0\varphi_0(k,r) \equiv \left( -\frac{d^2}{dr^2} + V_0(r) \right) \varphi_0(k,r) = k^2 \varphi_0(k,r), \tag{5}$$

whose solutions $\varphi_0(k,r)$ are known, analytically or numerically. These solutions allow one to construct a new Schrödinger equation for the same orbital momentum,

$$H_1\varphi_1(k,r) \equiv \left( -\frac{d^2}{dr^2} + V_1(r) \right) \varphi_1(k,r) = k^2 \varphi_1(k,r), \tag{6}$$

whose solutions are analytically expressed in terms of $\varphi_0(k,r)$ by

$$\varphi_1(k,r) = A_0^- \varphi_0(k,r). \tag{7}$$

The linear operator $A_0^-$ satisfies the characteristic intertwining relation of transformation operators [16],

$$A_0^- H_0 = H_1 A_0^-. \tag{8}$$

Here, $A_0^-$ is the first-order differential operator,

$$A_0^- = -\frac{d}{dr} + W(r), \tag{9}$$

where $W(r)$ is called the superpotential. With this form, Eq. (8) provides

$$V_1(r) = V_0(r) - 2\frac{d}{dr} W(r) \tag{10}$$

and a second-order linear differential equation for the superpotential. Equation (5) implies that the general solution of this equation is

$$W(r) = \frac{\varphi_0'(\kappa,r)}{\varphi_0(\kappa,r)}, \tag{11}$$

which depends on two independent variables: an energy $\mathcal{E} = \kappa^2$ and a ''shape parameter'' which determines the shape of the factorization solution $\varphi_0(\kappa,r)$. Notice that the normalization of $\varphi_0(\kappa,r)$ does not play any role in Eq. (11).

With the transformation operators (9), $H_0$ and $H_1$ are supersymmetric partners; i.e., they can be factorized as $H_0 = A_0^+ A_0^- + \mathcal{E}$ and $H_1 = A_0^- A_0^+ + \mathcal{E}$, where $A_0^+$ is the adjoint operator of $A_0^-$. The energy $\mathcal{E}$ is called the factorization energy, and the solution $\varphi_0(\kappa,r)$ is called the factorization solution. In applications of supersymmetry, the factorization energy is generally real ($\kappa$ is purely imaginary), whereas we shall allow this parameter to be complex.

We now examine which kind of factorization energies and solutions are necessary to solve the singular inverse problem. In general, four types of combined boundary conditions (at the origin and at infinity) are possible for the factorization solution $\varphi_0(\kappa,r)$, corresponding to four types of transformation. Each transformation type has a well-known effect on the potential spectrum [14]. When the solution is normalizable (regular at the origin and at infinity), the transformation removes the corresponding bound state from the spectrum. When the solution is neither regular at the origin nor at infinity, the transformation adds a bound state to the spectrum. In general, these two transformations are applied with real factorization energies to Hamiltonians involving real potentials.[1] In this case, the factorization solution can be chosen to be real, and consequently the transformed potential is also real. Whereas these two transformation types (respectively denoted by $T_1$ and $T_2$ in Ref. [15], and by $T_+^+$ and $T_-^-$ in Ref. [8]) are essential to modify the bound spectrum of potentials, they are of no interest here since we deal with potentials without bound spectrum.

The remaining two types of transformation, which do not modify the bound spectrum, will both be used in the following. When the factorization solution is regular at the origin and exponentially increasing at infinity (respectively singular at the origin and exponentially decreasing at infinity), it is denoted by $\varphi^L(\kappa,r)$ for *left* regular [respectively $\varphi^R(\kappa,r)$ for *right* regular] and the transformation by $T^L$ (respectively

[1] In recent works on complex optical potentials [17,12], complex factorization energies are employed.

$T^R$). In Ref. [15], this transformation is denoted by $T_3$ (respectively $T_4$), while in Ref. [8] it is denoted by $T^0_-$ (respectively $T^0_+$). In the following, superscripts thus provide the type of factorization solution, while subscripts are reserved to numbering Schrödinger equations, potentials, and solutions of equations. When solving the singular inverse problem, both transformations may be used with complex factorization energies. Consequently, the transformed potentials may also be complex; however, as will be seen in the next section, successive transformations can be used to derive a real final potential. Since we deal with potentials without a bound state, both $L$ and $R$ solutions have no node at finite distance. Consequently, the supersymmetric transformations do not introduce any singularity in the potential at finite distance, since the superpotential $W(r)$ given in Eq. (11) has no singularity except possibly at $r=0$.

The singularity of the potential at the origin is modified by the supersymmetric transformations: If the initial potential $V_0(r)$ satisfies

$$V_0(r) \underset{r\to 0}{\to} \frac{\nu_0(\nu_0+1)}{r^2}, \tag{12}$$

where $\nu_0=l$ for a regular potential and $\nu_0>l$ for a repulsive singular potential, an $L$ (respectively $R$) solution behaves like $r^{\nu_0+1}$ (respectively $r^{-\nu_0}$) for $r\to 0$. A series expansion of Eqs. (10) and (11) then implies that the transformed potential $V_1(r)$ satisfies

$$V_1(r) \underset{r\to 0}{\to} \frac{\nu_1(\nu_1+1)}{r^2}, \tag{13}$$

with $\nu_1=\nu_0+1$ (respectively $\nu_1=\nu_0-1$). In this article, we limit ourselves to $\nu\geqslant 0$ potentials; hence, we shall not apply a $T^R$ transformation to a potential with $\nu_0<1$ (this case is discussed elsewhere [7]).

The asymptotic behavior of the initial potential reads

$$V_0(r) \underset{r\to\infty}{\to} \frac{2\eta(k)k}{r}+\frac{l(l+1)}{r^2}, \tag{14}$$

where $\eta(k)=Z_1Z_2/2k$ is the dimensionless Sommerfeld parameter ($e=4\pi\epsilon_0=1$). Both $L$ and $R$ solutions then behave as

$$\varphi_0(\kappa,r) \underset{r\to\infty}{\to} e^{-i\kappa r+i\eta(\kappa)\ln(2i\kappa r)}[1+\epsilon_0(r)], \tag{15}$$

where $\kappa$ is chosen to lie in the upper (respectively lower) half $k$ plane for an $L$ (respectively $R$) solution in order to ensure the appropriate asymptotic behavior. The function $\epsilon_0(r)$ tends to zero asymptotically, at least as fast as $r^{-1}$; particular cases are discussed in the next section. Equations (10), (11), (14), and (15) imply that the transformed potential behaves asymptotically as

$$V_1(r) \underset{r\to\infty}{\to} \frac{2\eta(k)k}{r}+\frac{l(l+1)}{r^2}+\frac{2i\eta(\kappa)}{r^2}-2\frac{d^2\epsilon_0(r)}{dr^2}. \tag{16}$$

TABLE I. Main properties of supersymmetric transformations used for solving the singular inverse problem: location of additional $S$-matrix pole, modification of the asymptotic value of the phase shift, and modification of the potential singularity at the origin.

| Transformation | $S$-matrix pole | Phase shift | Singularity |
|---|---|---|---|
| $T^L$ (left regular) | $\mathrm{Im}\kappa>0$ | $\delta_1(\infty)=\delta_0(\infty)-\frac{\pi}{2}$ | $\nu_1=\nu_0+1$ |
| $T^R$ (right regular) | $\mathrm{Im}\kappa<0$ | $\delta_1(\infty)=\delta_0(\infty)+\frac{\pi}{2}$ | $\nu_1=\nu_0-1$ |

When no Coulomb term is present, the Sommerfeld parameter is zero, and the difference between $V_1$ and $V_0$ decreases faster than $r^{-2}$ at infinity. We shall see later that the $2i\eta r^{-2}$ term of Eq. (16) can be canceled when successive transformations are applied, even in the presence of a Coulomb interaction. The $r^{-2}$ term in the asymptotic form of both the initial and final potentials is then clearly related to the orbital momentum $l$, which is the same for both potentials.[2]

Equation (7) provides a relation between scattering states of $V_0$ and $V_1$. The asymptotic form of this equation, combined with Eqs. (9), (11), and (15), relates the phase shifts of $V_0$ and $V_1$, namely,

$$\delta_1(k)=\delta_0(k)+\arctan\frac{k}{i\kappa}. \tag{17}$$

When $\kappa$ is purely imaginary ($\mathcal{E}$ purely real), this formula reduces to the expression of Ref. [15], up to a difference of $\pi/2$ due to a different choice of the $l$ value for the final potential (see footnote 2). For the sake of simplicity, we make in this article the phase convention $\delta(0)=0$, as in Refs. [11] and [18] in the absence of a bound state. The potential singularity at the origin is then directly related to the asymptotic value of the phase shift.

From Eq. (17), the $S$ matrices are related by

$$S_1(k)=S_0(k)\frac{\kappa+k}{\kappa-k}. \tag{18}$$

A supersymmetric transformation thus introduces an $S$-matrix pole at $\kappa$. The main characteristics of the $T^L$ and $T^R$ transformations are summarized in Table I. One can verify that the phase-shift modification is in agreement with the generalized Levinson theorem (3) and with the modification of singularity (13) at the origin.

Formula (18) can also be obtained from the modification of the Jost function by supersymmetric transformations. In

[2]In Ref. [15], the orbital momentum is said to change, in contradiction with the fact that the angular part of the wave function remains unchanged. This interpretation may have several origins: (i) the modification of the singularity at the origin [Eq. (13)] or (ii) the shape invariance of the Coulomb potential, for which removing the ground state of a given partial wave $l$ with a single supersymmetric transformation precisely leads to the Coulomb potential of the partial wave $l+1$.

the Appendix, we express the $S$ matrix of a singular potential in terms of its Jost function by

$$S(k)=(-1)^{\nu-l}\frac{F(-k)}{F(k)}, \tag{19}$$

and we show that the modifications of the Jost function by supersymmetric transformations read

$$F_1(k)=F_0(k)\ \frac{k}{\kappa+k}\quad (T^L\ \text{transformation},\ \mathrm{Im}\kappa>0), \tag{20}$$

$$F_1(k)=F_0(k)\ \frac{-\kappa+k}{k}\quad (T^R\ \text{transformation},\ \mathrm{Im}\kappa<0). \tag{21}$$

Equations (19)–(21) lead to Eq. (18). Since the multiplicative factors in Eqs. (20) and (21) do not vanish in the upper half $k$ plane, no bound state is introduced by $T^L$ and $T^R$ transformations. The $S$-matrix poles in the upper half $k$ plane, introduced by $T^L$ transformations, correspond to poles of the Jost function in the lower half $k$ plane. This confirms that these transformations do not modify the bound spectrum, as stated above.

## III. ITERATION OF SUPERSYMMETRIC TRANSFORMATIONS

Supersymmetric transformations can be iterated: Factorizing Eq. (6) corresponding to $V_1$ can in turn give a new potential $V_2$, and so on. In some cases, the final potential $V_M$ resulting from $M$ transformations and its solutions can be expressed by compact formulas in terms of the initial solutions $\varphi_0(k,r)$ only. These cases are reviewed for the full line problem in Ref. [19] and the formulas can be transposed to the radial problem. We only mention here the case of interest for solving the singular inverse problem. Let $\mathcal{E}_1,\ldots,\mathcal{E}_M$ with $\mathcal{E}_m=\kappa_m^2$ be $M$ distinct factorization energies, $\varphi_{m-1}(\kappa_m,r)$ be the corresponding $L$ or $R$ factorization solutions, and $\varphi_0(\kappa_m,r)$ be the solutions of the initial equation of the same type. As mentioned before, subscripts number Schrödinger equations. The final potential reads, by repeated application of Eqs. (10) and (11),

$$V_M(r)=V_0(r)-2\frac{d}{dr}\sum_{m=1}^{M}\frac{\varphi'_{m-1}(\kappa_m,r)}{\varphi_{m-1}(\kappa_m,r)}, \tag{22}$$

and can be expressed in terms of solutions from the initial equation [19–21] as

$$V_M(r)=V_0(r)-2\frac{d}{dr}\frac{W'[\varphi_0(\kappa_1,r),\ldots,\varphi_0(\kappa_M,r)]}{W[\varphi_0(\kappa_1,r),\ldots,\varphi_0(\kappa_M,r)]}, \tag{23}$$

where $W$ is the Wronskian of the different solutions and $W'$ is its derivative with respect to $r$. The solutions of the corresponding Hamiltonian read

$$\varphi_M(k,r)=\frac{W[\varphi_0(k,r),\varphi_0(\kappa_1,r),\ldots,\varphi_0(\kappa_M,r)]}{W[\varphi_0(\kappa_1,r),\ldots,\varphi_0(\kappa_M,r)]}. \tag{24}$$

The final phase shift and $S$ matrix read, by iteration of Eqs. (17) and (18),

$$\delta_M(k)=\delta_0(k)+\sum_{m=1}^{M}\arctan\frac{k}{i\kappa_m} \tag{25}$$

and

$$S_M(k)=S_0(k)\prod_{m=1}^{M}\frac{\kappa_m+k}{\kappa_m-k}. \tag{26}$$

For a real potential, the $S$ matrix has to be unitary; this is the case if and only if the poles are symmetric with respect to the imaginary $k$ axis.

The asymptotic difference between the potentials is, by repeated application of Eq. (16),

$$V_M(r)-V_0(r)\underset{r\to\infty}{\to}\frac{2i}{r^2}\sum_{m=1}^{M}\eta(\kappa_m)-2\sum_{m=1}^{M}\frac{d^2\epsilon_{m-1}(r)}{dr^2}. \tag{27}$$

When the poles are symmetric with respect to the imaginary $k$ axis, the first term appearing in the right-hand side of this equation is purely real. Since we are interested in potentials decreasing faster than $r^{-2}$ at infinity, this term should vanish. Of course, it disappears when the potential contains no Coulomb term. Moreover, when the initial potential is short ranged, i.e., exponentially decreasing at infinity, the $\epsilon_{m-1}(r)$ functions are also exponentially decreasing. Consequently, the last term of Eq. (27) decreases exponentially, and the initial and final potentials are both short ranged; this implies that they both possess an effective-range expansion [22]. This will be used in the $np$ case discussed in next section.

The situation is more complicated for a repulsive-Coulomb plus short-range initial potential. In this case, the Coulomb effective-range expansion reads [23]

$$\frac{2\pi\eta k}{e^{2\pi\eta}-1}\cot\delta_0+2k\eta h(\eta)\underset{k\to0}{\to}-\frac{1}{a}+\frac{r_0}{2}k^2, \tag{28}$$

where we choose $l=0$ for simplicity. In this expression, $a$ is the scattering length, $r_0$ is the effective range, and $h(\eta)=\mathrm{Re}\Psi(1+i\eta)-\ln\eta$, where $\Psi$ is the digamma function [24]. In Ref. [23], the existence of an effective-range expansion (28) is shown to be related to the short-range character of the additional potential. When such an expansion exists, all the coefficients of a Taylor expansion about zero energy of the phase shift vanish, as can be seen with Eq. (28). Here, for a repulsive-Coulomb plus short-range initial potential $V_0$, the $\epsilon_{m-1}(r)$ functions in Eq. (27) are of order $r^{-1}$, so that in general the final potential has an $r^{-3}$ tail. Consequently, the effective-range expansion (28) is not valid after the transformation. In fact, Eq. (25) shows that a Taylor expansion of the phase-shift difference $\delta_M-\delta_0$ exists about zero energy. As suggested by Eq. (27), when the sum of $\kappa_m^{-1}$ is zero, the first-order term of the expansion and consequently the slope of $\delta_M-\delta_0$ at the origin vanish. The next coefficients of the Taylor expansion are in general different

from zero and the behavior of the physical phase shift cannot be perfectly reproduced at low energies.

The appearance of long-range terms in the inversion potential in the presence of a Coulomb interaction is a drawback of the supersymmetric method but also of all inversion methods based on rational expansions (26) of the $S$ matrix. However, in practice, this drawback is not really important: The long-range term in the potential tail can be made small, and an *approximate* effective-range expansion can be found when the energies are not very small. This is for instance the case in the $pp$ inversion of Sec. IV B.

An approximate solution of the singular inverse problem can be based on Eq. (26). The first step consists in finding the $\kappa_m$ poles, symmetric with respect to the imaginary $k$ axis, giving the best reproduction of the ''experimental'' phase shift. The second step is the inversion itself, i.e., the construction of the unique singular potential from those poles. Let us denote by $M^+$ (respectively $M^-$) the number of poles in the upper (respectively lower) half $k$ plane. In previous inversion schemes [25–27], the poles are constrained to satisfy the additional condition $M^+=M^-$, in order to obtain a regular potential. The main novelty of our method is that $M^+$ is allowed to be larger than $M^-$. Consequently the potential can have a repulsive singular core with parameter

$$\nu_M = l + M^+ - M^- . \tag{29}$$

Equation (26) also appears in the theory of Bargmann potentials [1]. When the numbers of poles in the upper and lower half $k$ planes are equal, Eqs. (23) and (24) reduce to the usual Bargmann formulas, with the help of the initial Schrödinger equation (5).

Following Refs. [25–27], the $S$ matrix is approximated by

$$S(k) \approx S_M(k) = S_0(k)\,\frac{1+P_M(-k)}{1+P_M(k)}, \tag{30}$$

where $S_0(k)$ is the $S$ matrix of the initial or reference potential $V_0$, and $P_M(k)$ is a polynomial of degree $M$, providing the $S$-matrix poles. The coefficients can be found by minimizing

$$\chi^2 = \sum_j^{\text{data}} \frac{|S(k_j)[1+P_M^{(n)}(k_j)] - S_0(k_j)[1+P_M^{(n)}(-k_j)]|^2}{|1+P_M^{(n-1)}(k_j)|^2 \Delta_j^2}, \tag{31}$$

where $\Delta_j$ is the error on the experimental value $S(k_j)$, and $n$ is an iteration index. This nonlinear problem is made linear by the following iteration scheme. Choosing $P_M^{(0)}(k)=0$ provides a linear system for the coefficients of $P_M^{(1)}(k)$. This system can be solved, for instance, by the singular-value-decomposition method [28]. The solution $P_M^{(1)}(k)$ introduced in Eq. (31) provides in turn a linear system for the coefficients of $P_M^{(2)}(k)$, and so on. This iteration process strongly restricts the number of nonphysical poles located very close to the real axis, which are often obtained after the first iteration [27]. In the cases treated in the application, 20 iterations are typically needed to move these poles away from the real axis. Let us, however, notice that these poles cannot *all* be moved away when $M$ is taken too large; consequently, different $M$ values have to be tried in order to find the ''cheapest'' fit. In this automatic minimization, the numbers $M^+$ and $M^-$ (and hence the singularity of the potential) cannot be chosen *a priori*: They are directly provided by the system resolution.

TABLE II. Elastic phase shifts of the nucleon-nucleon $^1S_0$ scattering, as functions of the laboratory energy $E_{\text{lab}}$. Single-energy (multienergy at 0.1 MeV) phase shifts $\delta_{\text{expt}}$ from Ref. [29] and phase shifts $\delta_M$ of Eq. (25).

| $E_{\text{lab}}$ (MeV) | $\delta_{\text{expt}}^{np}$ (Ref. [29]) (deg) | $\delta_5^{np}$ (deg) | $\delta_{\text{expt}}^{pp}$ (Ref. [29]) (deg) | $\delta_7^{pp}$ (deg) |
|---|---|---|---|---|
| 0.1 | $38.43\pm0.10$ | 38.4 | $2.30\pm0.10$ | 2.2 |
| 5 | $63.70\pm0.10$ | 63.5 | $54.36\pm0.10$ | 54.2 |
| 10 | $59.52\pm0.10$ | 59.9 | $53.94\pm0.10$ | 54.3 |
| 15 | $56.73\pm0.47$ | 56.7 | $52.39\pm0.47$ | 52.4 |
| 25 | $51.67\pm0.11$ | 51.5 | $48.31\pm0.11$ | 48.1 |
| 50 | $41.87\pm0.06$ | 41.8 | $39.19\pm0.06$ | 39.1 |
| 75 | $33.68\pm0.26$ | 34.4 | $31.28\pm0.26$ | 32.0 |
| 100 | $27.55\pm0.34$ | 28.0 | $25.37\pm0.34$ | 25.8 |
| 150 | $17.08\pm0.31$ | 17.2 | $15.32\pm0.31$ | 15.5 |
| 200 | $8.57\pm0.34$ | 8.3 | $7.20\pm0.34$ | 6.9 |
| 250 | $0.62\pm0.85$ | 0.7 | $-0.44\pm0.85$ | $-0.3$ |
| 300 | $-5.73\pm0.30$ | $-5.7$ | $-6.54\pm0.30$ | $-6.5$ |
| 350 | $-10.93\pm0.54$ | $-11.2$ | $-11.55\pm0.54$ | $-11.8$ |

Let us finally discuss the inversion process itself. In previous works [25–27], the inversion is done by solving the Gel'fand-Levitan or Marchenko integral equation, which reduces to a linear system in the case of an $S$ matrix of the form (26). In the present method, one can choose either a direct (and explicit) derivation of the potential by Eq. (23), or an iterative construction based on Eq. (22) which makes possible a control of the potential at each step.

## IV. APPLICATION TO NUCLEON-NUCLEON ELASTIC SCATTERING

### A. Neutron-proton $^1S_0$ elastic scattering

As a first example of our method, we invert phase shifts of the neutron-proton ($np$) elastic scattering in the $^1S_0$ channel. The data are the single-energy phase shifts of the Virginia group [29] below the pion threshold, i.e., 12 points between 5 and 350 MeV, with error bars. They are given in Table II. In order to reproduce the low-energy behavior of the phase shift, we add some low-energy data from the multienergy analysis of the same group, for which no error bar is provided. In both the $np$ and $pp$ (see next subsection) cases, we obtain good results with only one additional point at 0.1 MeV, with an error bar of 0.1° chosen by us. Another possibility would be to directly add to the fit the contributions of the scattering length and effective range, since they can be expressed linearly in terms of the first coefficients of polynomial $P_M(k)$. We prefer to use the first method, which can be generalized to the $pp$ case.

The reference potential is chosen to be $V_0(r)=0$, with $S_0(k)=1$. Another possible choice is the one-pion exchange potential (OPEP), but we prefer to compare our potential with the OPEP. The smallest number of poles providing an accurate fit to the data is 5. Higher numbers do not improve

TABLE III. Real and imaginary parts of the $S$-matrix poles $\kappa_m$ obtained by fitting the phase shifts of Table II for the $np$ (first column) and $pp$ (third column) $^1S_0$ elastic scatterings. The second column displays the poles of Ref. [25] in the $np$ case.

| $np$ (this article) | | $np$ (Ref. [25]) | | $pp$ (this article) | |
|---|---|---|---|---|---|
| Re$\kappa$ (fm$^{-1}$) | Im$\kappa$ (fm$^{-1}$) | Re$\kappa$ (fm$^{-1}$) | Im$\kappa$ (fm$^{-1}$) | Re$\kappa$ (fm$^{-1}$) | Im$\kappa$ (fm$^{-1}$) |
| $\pm 1.313$ | 1.453 | $\pm 1.872$ | 1.679 | $\pm 1.347$ | 1.499 |
| | 0.581 | | 1.024 | | 0.729 |
| | $-0.040$ | | $-0.042$ | | 0.080 |
| | $-0.837$ | | $-2.953$ | $\pm 0.073$ | $-0.077$ |
| | | | $-70.904$ | | $-1.100$ |

the fit much, and generally provide the same five poles together with other poles with weak physical interest, i.e., very close to the real axis or very remote from the complex $k$ plane origin. An example is presented below. The obtained values for the phase shift are given in Table II, while the poles are listed in Table III. The 13 phase shifts are reproduced by the rational expansion (26) of the $S$ matrix with a $\chi^2$ of 35. Let us notice that the 10 MeV and 75 MeV data (or their error bars) are responsible for about two-thirds of this $\chi^2$, and that the Virginia multienergy values at these energies are 60° and 34.51°, which are much closer to the present values. The rational expansion of the $S$ matrix thus seems to have a smoothening effect similar to the multienergy calculation. This suggests that such rational expansions could directly be used in multienergy phase-shift parametrizations. The rational expression (26) of the $S$ matrix also provides the scattering length and effective range presented in Table IV (for example, $a=i\Sigma\kappa_m^{-1}$). Our results are in very good agreement with values deduced from experiment. Let us emphasize that these *two* quantities are obtained with only *one* phase shift below 5 MeV in the fit.

Let us now examine the obtained poles. One of the poles in Im$k<0$ is very close to the real axis; it corresponds to a virtual state of the $np$ system. Because of this pole, the phase shift rapidly increases near the origin, with a positive slope at zero energy (see Ref. [12] for a general discussion of the influence of an $S$-matrix complex pole on the phase shift). The numbers of poles $M^+=3$ and $M^-=2$ imply that the phase shift tends to $-\pi/2$ asymptotically, in agreement with Eqs. (4) and (29), and that the $S$ matrix tends to $-1$. This may seem to be physically surprising, but one has to remember that the potential found is only meant to reproduce single-channel elastic phase shifts, while other channels appear at energies higher than the pion threshold. To our knowledge, no simple *physical* argument compels the $S$ matrix to tend to 1 at infinity: the reasons evoked in textbooks are always related to a particular *mathematical* description, namely, a sufficiently regular potential. Our aim is here to find as simple as possible a model in the purely elastic energy range.

TABLE IV. Scattering length $a$ and effective range $r_0$ of the inversion potentials and recommended values.

| | $a$ (fm) | $r_0$ (fm) |
|---|---|---|
| $np$ (this article) | $-23.723$ | 2.70 |
| $np$ (Ref. [31]) | $-23.721\pm 0.020$ | $2.658\pm 0.062$ |
| $pp$ (this article) | $-7.8\pm 0.1$ | $2.8\pm 0.1$ |
| $pp$ (Ref. [32]) | $-7.8196\pm 0.0026$ | $2.790\pm 0.014$ |

First we compare our $S$-matrix expansion with that of Ref. [25], where a similar inversion is treated with a standard method and where the $S$-matrix poles are explicitly given. The data used in Ref. [25] are the real parts of the Virginia multienergy phase shifts, with constant error bars, between 0 and 1100 MeV. The obtained poles are reproduced in Table III for comparison with ours. The virtual state is very close to the present one. The next four poles are qualitatively similar to ours in spite of the different data sets used. In Ref. [25], one additional pole in the lower half $k$ plane, which is very remote from the other ones, has nearly no influence on the phase shift in the low-energy region. It only makes the phase shift tend to zero at very high energies and regularizes the potential at the origin. The simplicity argument evoked above naturally leads to eliminate this kind of pole in the fit of the phase shift and to accept a singular potential. Moreover, the poles of Ref. [25] indirectly confirm that the best fit of the data is obtained with five poles: For $M=6$, the automatic minimization clearly provides a $5+1$ structure in the

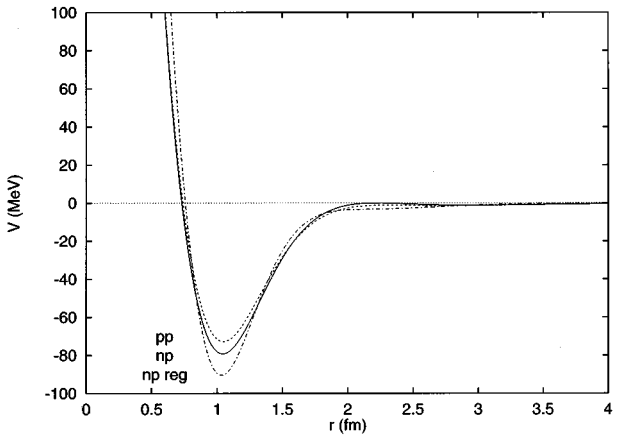


FIG. 1. Singular potentials obtained by inversion for the $np$ $^1S_0$ elastic scattering (solid line) and for the $pp$ $^1S_0$ elastic scattering (dashed line), and regular $np$ $^1S_0$ potential of Ref. [25] (dash-dotted line).

pole distribution, with one pole out of the physically interesting energy range.

The potential obtained by supersymmetric inversion, displayed in Figs. 1–3, has a singular repulsive core of the form $2r^{-2}$, in agreement with Eq. (29). Since $V_0(r)=0$, an $L$ solution is a hyperbolic sine function and an $R$ solution is a decreasing exponential, and the explicit form (23) of the real $np\ ^1S_0$ potential reads

$$V_5(r)=-2\frac{d^2}{dr^2}\ln W\{\sin[(1.313+1.453i)r],\sin[(-1.313+1.453i)r],\sinh(0.581r),\exp(-0.040r),\exp(-0.837r)\}, \tag{32}$$

where the Wronskian is purely imaginary because of the symmetry of the poles. This potential reduces to a ratio of linear combinations of real and complex exponentials corresponding to the poles of the upper half $k$ plane. This formula can be thought of as a parametrization of the $np\ ^1S_0$ central interaction with five real parameters. The potential of Ref. [25], represented in Fig. 1, can also be written with a formula similar to Eq. (32), but containing six functions.

Figure 1 shows that our potential and the potential of Ref. [25] have a similar shape, as could be foreseen from the similarity of their poles. The latter potential also seems to be singular at the origin. In fact, the remote pole regularizes it at very high energies: $V(0)$ is equal to 418 000 MeV. Beyond this large energy, the corresponding phase shift tends to zero, while it continues to tend towards $-\pi/2$ for ours. Both potentials have a deep well around 1 fm. As shown in Figs. 2 and 3, our potential has also a shallow well of $-1.2$ MeV around 3 fm and an exponential tail close to the OPEP beyond 6 fm.

To test the stability of the potential shape while varying the data, we also performed calculations with a set of 116 multienergy phase shifts in the same energy range, and the obtained potential is very close. In particular, the shallow well is still present. The multienergy data also allowed us to continuously vary the energy interval; the obtained potentials are similar for all energy intervals between 0–300 MeV and 0–450 MeV. When additional real parts of complex phase shifts are introduced beyond 450 MeV, the reproduction of the real phase shifts below pion threshold deteriorates. In particular, effective-range parameters become less good. Simultaneously, the shape of the potential begins to change: The shallow well reduces to a kind of plateau at about $-3$ MeV around 2 fm, and the potential tail vanishes faster than the OPEP. This is, for instance, the case with the potential of Ref. [25], since these authors invert data up to 1100 MeV. In more recent works [26,27], these authors also limit the energy range and obtain potentials with the same kind of shallow structure as here, with a correct asymptotic behavior and with good effective-range parameters. It may be more physical to fit real phase shifts below the pion threshold even if, for some purposes, inversion of higher-energy data seems to be necessary [30].

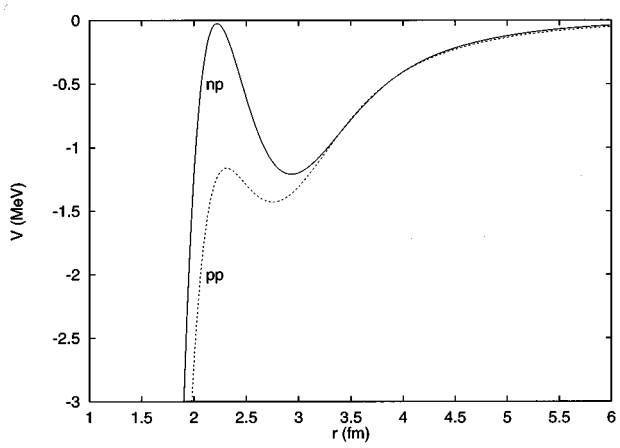


FIG. 2. Shallow structure of the singular potentials obtained by inversion in the $np$ (solid line) and $pp$ (dashed line) cases.

### B. Proton-proton $^1S_0$ elastic scattering

We perform the same calculation in the $pp$ case in order to test our method in presence of a Coulomb potential. Adding a Coulomb term to the potential obtained in Sec. IV A only provides a qualitative reproduction of the phase shift, typically with an error of 5° An inversion method is thus necessary to obtain a quantitative reproduction of the data.

The data are chosen in exactly the same manner as in the $pp$ case : twelve single-energy phase shifts of Ref. [29], displayed in Table II, and one multienergy point at 0.1 MeV

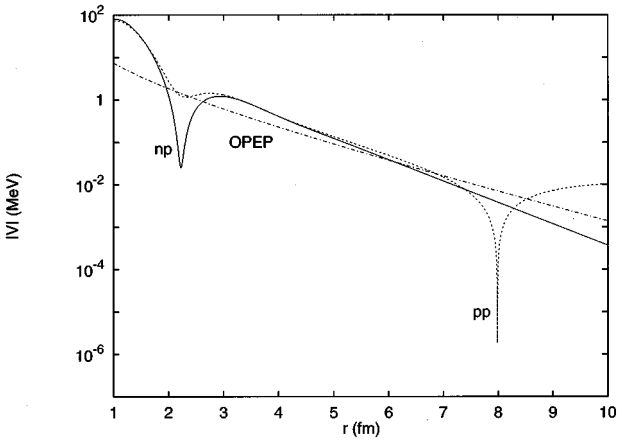


FIG. 3. Asymptotic behavior of the $np$ (solid line) and $pp$ (dashed line) singular potentials, in logarithmic scale. The OPEP potential $-14.8\exp(-0.697r)/r$ MeV is represented by a dash-dotted line.

with an assumed error of 0.1°. The reference potential $V_0$ is now a Coulomb potential, regularized as a sphere-sphere potential below 1.6 fm. The reference $S$ matrix $S_0$ is thus calculated numerically. The results obtained with a nonregularized Coulomb potential or with other regularized potentials are very close to those described below.

The rational factor in the $S$ matrix is imposed to be of order $k^2$ near the origin (the coefficient of $k$ in $P_M$ is forced to zero). This is equivalent to canceling the sum of the $\kappa_m^{-1}$. The phase-shift slope at the origin and the $r^{-2}$ term in Eq. (27) then vanish. The obtained poles are displayed in Table III. The quality of the fit is similar to that of the $np$ case. The main inaccuracies also correspond to the 10 MeV and 75 MeV data. The difference $M^+ - M^-$ equals unity as in the $np$ case, which means that the phase shift also tends to $-\pi/2$ at infinity and that the potential has a repulsive core of the form $2r^{-2}$.

The pole locations are similar to the ones of the $np$ case, except for the virtual state, which is replaced by three poles close to the origin. The two poles in the lower half $k$ plane correspond to a narrow resonance, and the combined effect of the three poles on the phase shift is a nearly vanishing slope at the origin, followed by an increase around 1 MeV.

In the $pp$ case, the explicit expression of the potential, corresponding to Eq. (32) of the $np$ case, would contain solutions of the regularized Coulomb potential rather than simple exponential or hyperbolic sine functions. These solutions match Whittaker functions in the external region and parabolic cylinder functions in the internal region [24]. They are continuous as well as their first derivatives. Using the initial Schrödinger equation (5), their higher-order derivatives can be expressed in terms of these functions and of their first-order derivatives. The Wronskian of Eq. (23) can be calculated as in Ref. [21]. The additional potential $V_M - V_0$ is shown in Figs. 1–3; it is qualitatively close to the $np$ potential, as expected from charge independence. Its tail is not exponentially decreasing; however, Fig. 3 shows that an exponential decrease is simulated up to 7 fm where the potential is already very small. Beyond 7 fm, a node occurs. The $r^{-3}$ term becomes dominant beyond 150 fm only. This shows that the method can simulate a short-range behavior at physically important distances.

The long-range tail in the final potential implies that no exact effective-range expansion exists. However, we can fit the effective-range parameters $a$ and $r_0$ to phase shifts $\delta_M$ calculated at two low energies. By varying these energies, we can verify whether an approximate effective-range expansion exists in some energy interval, and estimate its coefficients. With energies between 2.5 and 7 MeV, we obtain the coefficients displayed in Table IV. However, at lower energies, the phase shift is not perfectly reproduced. The inaccuracy is maximum near 0.5 MeV but does not exceed 2°. With more poles in the expansion and more low-energy data to constrain them, it should be possible to reduce this inaccuracy but let us emphasize again that a perfect agreement at very low energies is not possible. Anyway, when the tail of the potential is well simulated, the effective-range expansion is well approximated in some energy range.

Calculations with multienergy phase shifts lead to the same conclusions as in the $np$ case. In particular, when higher-energy data are added, the second well also becomes a plateau and the data below pion threshold are less well reproduced. The same inversion has been perfomed with a standard method and regular potentials in Ref. [27].

## V. CONCLUSION

Singular potentials should become a useful tool for inversion methods, since they only depend on scattering data. A general inversion method at fixed orbital momentum can now be decomposed into two complementary but clearly separated physical problems: deriving a potential from phase shifts and choosing the most appropriate bound spectrum for this potential. Supersymmetric transformations provide a powerful way of solving each of these problems. The first step constitutes the singular inverse problem, introduced and treated in this article. Other approaches can probably also be extended to solve this singular inverse problem.

The first step of our inversion scheme starts with the choice of a reference potential and with a parametrization of the $S$ matrix under the form (26), with different numbers of poles in the upper and lower half $k$ planes. The number of poles should, however, not be larger in the lower half plane. In this respect, a fitting method allowing a definite choice of the number of poles in both half planes might be helpful. The method presented here *deduces* these numbers from the fitting scheme for a given total number of poles. The potential corresponding to these poles, which is in general singular, is then obtained with single supersymmetric transformations. If the wave functions of the reference potential are known analytically, an analytical expression of this potential is also available.

In a second step, bound states can be added either for physical reasons or for reducing the singularity. This step is not indispensable. The phase-equivalent addition of physical bound states with given normalization constants can be performed with supersymmetric transformation pairs [7–10]. Such transformations reduce the singularity of the potential by 2 for each bound-state addition. The final potential can be regular, as in the traditional inverse problem. This is possible for an even singularity of the singular potential obtained after the first step, i.e., when the $S$ matrix tends to 1 at infinity. However, odd-singularity potentials are also possible if the best fit corresponds to an $S$ matrix tending to $-1$. In this second step, nonphysical bound states simulating forbidden states [3] can also be introduced in addition to physical ones. In some applications, this might lead to deep potentials independent of, or weakly dependent on, the orbital momentum. The study of this last point is in progress.

The application of our method to the nucleon-nucleon $^1S_0$ elastic scatterings leads to potentials with a singular repulsive core of the form $2r^{-2}$. The corresponding phase shifts tend to $-\pi/2$ at infinity; i.e., the $S$ matrix tends to $-1$. No obvious physical argument allows one to reject such potentials, since their definition is based on finite-energy ranges where a single channel is open. It would be interesting to evaluate off-shell properties of such potentials. The odd singularity makes impossible a regularization of these potentials by a phase-equivalent addition of a bound state simulating a forbidden state. Therefore, they cannot easily be compared with the deep nucleon-nucleon potential of Ref. [33]. Our singular potentials have good low-energy proper-

ties and are fairly close to the OPEP potential at large distances. In previous inversions of nucleon-nucleon phase shifts [25–27], the obtained potentials are in fact very close to singular potentials, even if the singularity is not allowed explicitly. In such a case, simplicity favors using a singular potential.

## ACKNOWLEDGMENTS

J.-M.S. is supported by the Fonds National de la Recherche Scientifique of Belgium. This text presents research results of the Belgian program on interuniversity attraction poles initiated by the Belgian-state Federal Services for Scientific, Technical and Cultural Affairs.

## APPENDIX

In this appendix, we first recall some formulas of scattering theory for singular potentials. Details and references can be found in Ref. [12] (see also Ref. [34] for analytical examples). We then deduce from those formulas the modification of the Jost solutions and Jost function by supersymmetric transformations.

For a given partial wave $l$, the Jost solutions of the radial Schrödinger equation follow the asymptotic behavior

$$f(k,r) \underset{r\to\infty}{\to} \exp[i\,\tfrac{1}{2}\nu\pi + ikr - i\,\eta(k)\ln(-2ikr)], \quad \text{(A1)}$$

where $\nu$ is the parameter of the singular repulsive core of the effective potential at the origin. The regular solution of the radial equation has a definite normalization at the origin,

$$\psi(k,r) \underset{r\to 0}{\to} \frac{r^{\nu+1}}{(2\nu+1)!!}. \quad \text{(A2)}$$

It can be expressed as a linear combination of the Jost solutions

$$\psi(k,r) = \tfrac{1}{2} i k^{-\nu-1} \exp[\epsilon\eta(k)\pi][F(k)f(-k,r) - (-1)^{\nu}F(-k)f(k,r)], \quad \text{(A3)}$$

where $\epsilon = \mathrm{sgn}\ \mathrm{Re}k$. This defines the Jost function $F(k)$, which also satisfies

$$F(k) = \frac{(-k)^{\nu}}{(2\nu-1)!!} \lim_{r\to 0} [r^{\nu} f(k,r)]. \quad \text{(A4)}$$

For real energies, $\psi(k,r)$ must behave asymptotically like $\sin[-\frac{1}{2}l\pi + kr - \eta(k)\ln(2kr) + \sigma^{l}(k) + \delta(k)]$, where $\sigma^{l}(k)$ is the Coulomb phase shift; this imposes the link (19) between the $S$ matrix and the Jost function.

Jost solutions are modified by supersymmetric transformations according to Eq. (7) but with a normalization fixed by Eq. (A1). Equations (9) and (11) then imply that

$$f_1(k,r) = \frac{i}{\kappa + k} \exp[i\,\tfrac{1}{2}(\nu_1 - \nu_0)\pi] A_0^{-} f_0(k,r). \quad \text{(A5)}$$

Below, we need the behavior of $f_1(k,r)$ near the origin. This is easy for a $T^L$ transformation ($\nu_1 = \nu_0 + 1$), remembering that Jost solutions are in general singular at the origin and behave like $r^{-\nu}$. For a $T^R$ transformation ($\nu_1 = \nu_0 - 1$), a higher-order expansion of the Jost solutions $f_0(k,r)$ and of the factorization solution $\varphi_0(\kappa,r)$ near the origin makes the calculation more complicated: The $r^{-\nu_0}$ term of Eq. (A5) vanishes and the $r^{-\nu_1} = r^{-\nu_0+1}$ term is needed.

Let us now consider the transformation of the Jost function. For a $T^L$ transformation, combining Eqs. (A4) and (A5) directly provides the modification (20) of the Jost function. For a $T^R$ transformation, it is simpler to determine the way the regular solution is modified by the transformation. The regular solution also transforms according to Eq. (7), but with its normalization fixed by Eq. (A2). The obtained relation

$$\psi_1(k,r) = -A_0^{-}\psi_0(k,r) \quad (T^R \text{ transformation}) \quad \text{(A6)}$$

combined with Eq. (A3) provides Eq. (21).

Let us mention here that formula (A6) is also valid in the case of a $T^L$ transformation, up to a normalization constant. Since $\psi_1(k,r)$ has to behave according to Eq. (A2), a higher-order expansion of the regular solution and of the factorization solution would be needed near the origin because the $r^{\nu_0+1}$ term of Eq. (A6) vanishes.

[1] K. Chadan and P. C. Sabatier, *Inverse Problems in Quantum Scattering Theory* (Springer, Berlin, 1977).
[2] R. G. Newton, *Scattering Theory of Waves and Particles* (Springer, New York, 1982).
[3] V. G. Neudatchin, V. I. Kukulin, V. L. Korotkikh, and V. P. Korennoy, Phys. Lett. **34B**, 581 (1971); B. Buck, H. Friedrich, and C. Wheatley, Nucl. Phys. **A275**, 246 (1977); W. Ihra and H. Friedrich, Phys. Rev. A **45**, 5278 (1992).
[4] K. Wildermuth and Y. C. Tang, in *A Unified Theory of the Nucleus*, edited by K. Wildermuth and P. Kramer (Vieweg, Braunschweig, 1977).
[5] P. Swan, Proc. R. Soc. London, Ser. A **228**, 10 (1955).
[6] D. Baye, Phys. Rev. Lett. **58**, 2738 (1987).
[7] D. Baye, J. Phys. A **20**, 5529 (1987).
[8] L. U. Ancarani and D. Baye, Phys. Rev. A **46**, 206 (1992).
[9] D. Baye, Phys. Rev. A **48**, 2040 (1993).
[10] D. Baye and J.-M. Sparenberg, Phys. Rev. Lett. **73**, 2789 (1994).
[11] P. Swan, Nucl. Phys. **46**, 669 (1963).
[12] J.-M. Sparenberg and D. Baye, Phys. Rev. C **54**, 1309 (1996).
[13] E. Witten, Nucl. Phys. **B188**, 513 (1981).
[14] C. V. Sukumar, J. Phys. A **18**, 2917 (1985).
[15] C. V. Sukumar, J. Phys. A **18**, 2937 (1985).
[16] B. M. Levitan, *Generalized Translation Operators and some of their Applications* (Israel Program for Scientific Translations, Jerusalem, 1964).

[17] D. Baye, G. Lévai, and J.-M. Sparenberg, Nucl. Phys. **A599**, 435 (1996).
[18] Z. R. Iwinski, L. Rosenberg, and L. Spruch, Phys. Rev. A **31**, 1229 (1985).
[19] J.-M. Sparenberg and D. Baye, J. Phys. A **28**, 5079 (1995).
[20] M. M. Crum, Q. J. Math. **6(2)**, 121 (1955).
[21] P. Deift and E. Trubowitz, Commun. Pure Appl. Math. **32**, 121 (1979).
[22] M. L. Goldberger and K. M. Watson, *Collision Theory* (Wiley, New York, 1964).
[23] H. van Haeringen, *Charged Particle Interactions, Theory and Formulas* (Coulomb Press, Leyden, 1985).
[24] *Handbook of Mathematical Functions*, edited by M. Abramowitz and I. A. Stegun (Dover, New York, 1970).
[25] M. Coz, J. Kuberczyk, and H. V. von Geramb, Z. Phys. A **326**, 345 (1987).
[26] Th. Kirst, K. Amos, L. Berge, M. Coz, and H. V. von Geramb, Phys. Rev. C **40**, 912 (1989).
[27] H. V. von Geramb and H. Kholhoff, in *Quantum Inversion Theory and Applications*, edited by H. V. von Geramb, Lecture Notes in Physics (Springer, Berlin, 1993), Vol. 427, p. 285.
[28] W. H. Press, B. P. Flannery, S. A. Teukolsky, and W.T. Vetterling, *Numerical Recipes, The Art of Scientific Computing* (Cambridge University Press, Cambridge, England, 1986).
[29] R. A. Arndt and L. D. Roper, *Scattering Analysis Interactive Dial-in SAID* (Virginia Polytechnic Institute, Blacksbury, 1996).
[30] H. F. Arellano, F. A. Brieva, M. Sander, and H. V. von Geramb, Phys. Rev. C **54**, 2570 (1996).
[31] L. Mathelitsch and B. J. VerWest, Phys. Rev. C **29**, 739 (1984).
[32] J. R. Bergevoet, P. C. van Campen, W. A. van der Sanden, and J. J. de Swart, Phys. Rev. C **38**, 15 (1988).
[33] V. I. Kukulin and V. N. Pomerantsev, Prog. Theor. Phys. **88**, 159 (1992).
[34] G. A. Natanzon, Teor. Mat. Fiz. **38**, 219 (1979) [Theor. Math. Phys. **38**, 146 (1979)].